Experiments and model on viscosity characteristic of emulsion of heavy fuel oil and water for fluidity improvement

Isamu Fujita [a,*] , Xiao Ma [b] , Masao Ono [b] and Hideyuki Shirota [b]

[a] National Institute of Maritime, Port and Aviation Technology, Port and Airport Research Institute, 3-1-1 Nagase, Yokosuka, Kanagawa, 239-0826,Japan

[b] National Institute of Maritime, Port and Aviation Technology, National Maritime Research Institute, 6-38-1 Shinkawa, Mitaka, Tokyo, 181-0004, Japan

* Corresponding author.
E-mail address: fujita@p.mpat.go.jp

Abstract

The background of this study is to develop a method to improve the fluidity of high viscosity oil left in sunken ships. We focused on emulsification to control the rheological properties of the oil. As a first step towards the goal, experiments and modeling were conducted to understand the viscosity properties of oil-water emulsions. In the experiments, oil-water emulsions were prepared using several surfactants to measure viscosity properties. The results showed a continuous change in viscosity with increasing water content as well as a discontinuous change in viscosity due to phase inversion that occurs at a certain water content. In the theoretical modelling, a new layer-stacking model was developed and applied to the experimental results. This model, though extremely simplifying the structure of the emulsion, was found to be able to well explain the continuous and discontinuous viscosity characteristics of the emulsion.

Key words

Emulsion, Viscosity, Surfactant, Phase inversion, Model, Heavy fuel oil

Nomemclature

Symbols

β : shear strain ratio/fraction
γ : shear strain
$\dot{\gamma}$: shear strain rate ($= \frac{d\gamma}{dt}$)
ϵ : porosity/void fraction in particle-packed layer
ϕ : volume fraction
μ : viscosity
τ : shear stress
Z : normalized Layer tickness

Subscripts

B : of component which constitues bulk layer
P : of component which mainly constitues paticle-packed layer
b : of/in bulk layer
e : of/in entire system
p : of/in paticle-packed layer
o : of oil

w : of water

1. Introduction

In the field of oil spill response, a counter measure to oil leakage from sunken ships is one of the most crucial issues. Historically, many ships have sunk with oil left in their fuel tanks. There were cases that a small amount of oil continued to leak for a long period of time, or leakage started after decades, which caused troublesome problems that could not be left unattended. It may be necessary to take measures by subsurface oil recovery from the sunken ship (Hansen,2014). In the deep sea or when the water temperature is low, the oil to be extracted has a high viscosity, which may makes the recovery mission difficult. To overcome this difficulty, some counter measure is required to improve fluidity of the high viscosity oil.

There were many studies on the pipeline flow so far. Among them, basic studies on multiphase flow of oil and water have been conducted for a long time (Russell,1959; Bunnwart,2004), and even in recent years, multiphase flow for high-viscosity oil has been attracting attention (Vuong,2009), reflecting the shift of oil production to high-viscosity oil. On the other hand, as a technology for dealing with spilled oil, several technologies for in-pipe transportation of high-viscosity oil, including W/O emulsified by weathering, have been proposed. These include the technique of forming CAF (Core Annular Flow) by adding water (Drieu,2003; I.Fujita,2009) and the method of adding a small amount of surfactant instead of water(I.Fujita,2011). These methods control the structure of flow in the pipe to reduce the pipe friction loss, however, are not suitable for improving the fluidity of a large mass of oil remaining inside the fuel tank of a wreck.

In oil recovery from the sunken ships, the fluidity of the oil inside the tank is important as well as in in the pipeline. For this purpose, bulk heating is one of the options easy to conceive. It, however, has disadvantages such as requiring a large amount of energy, poor heat transfer rate or heat dissipation into the cold water . Ono et al. tried to improve the flowability by the bulk heating using induction heating (M.Ono(1),2015; M.Ono(2),2015), but found that it was difficult to transfer heat deep into the tank to enhance the fluidity of the entire tank. Therefore, we needed to look for alternatives and focused on the improvement of fluidity by emulsification from a rheological point of view. Our original idea was to use a vapor explosion to simultaneously realize to disperse oil as fine particulates into water and to reach the effect deep in the tank (M.Ono,2018 ;Ono,2019). However, in order to achieve this, knowledge of emulsions composed of heavy fuel oil and water is not sufficient yet.

In this study, we investigate the viscosity properties of emulsions composed of heavy fuel oil and water in a basic system without thermal phenomena such as vapor explosion. In general, W/O emulsion is formed in nature, as is the case with spilled heavy oil, and viscosity increases, but in systems where surfactants are added, emulsions of various forms can be produced, which may lead to resolve the poor flowability problem.

In the following sections, experiments are conducted to measure the viscosity properties of oil-water emulsions with surfactants, and the results are analyzed using a newly proposed viscosity model and microscopic observations.

2. Experiments

2.1. Sample Preparation

This section describes the experimental procedure of viscosity measurement for water-oil emulsions system we conducted in the study. For the test oil, an oil called C fuel oil, which is widely distributed as fuel oil in Japan, was used. This oil is specified in the Japanese Industrial Standard (JIS) K2205 and corresponds to MFO (marine fuel oil) as an international designation. Its viscosity characteristic is shown in Fig.1. The measurements were carried out using a Brookfield B-type viscometer (DV-III Ultra) at a

temperature of 25°C.

As shown in Fig.2, test samples were prepared using the agent-in-oil method, whose procedure is as follows:

(1) Add chemical agent to the oil and stir for a while.
(2) Weigh a certain amount (100 or 200g) from sample (1).
(3) Weigh distilled water so that the desired water content is obtained, and add it to the sample (2).
(4) Stir sample (3) at a constant rate for 3 minutes.
(5) Deaerate sample (4) in a vacuum chamber for 3 minutes.

A household juicer mixer of which power was 160W, was used for stirring in the step (4). Three types of chemicals, AB-3000, OTP-75 and MYL-10 were used as additive chemical agents. AB-3000 was selected as a representative of the general type oil dispersant commercially available in Japan. OTP-75 is a 75% solution diluted with water and ethanol containing diethylhexyl sodium sulfosuccinate as a surfactant component, and is used for wetting, permeation, and dispersion. MYL-10 is PEG-10 laurate often used as hydrophilic emulsifier. The selection of these agents was based on Fujita's work on the decomposition of W/O emulsions(I.Fujita,2013). Test samples we prepared for the test are summarized in Table 1.

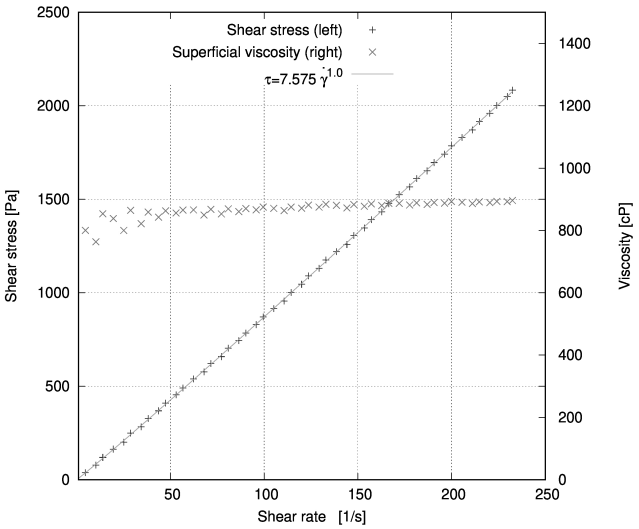

Figure 1 Viscosity of the test oil used for the experiment

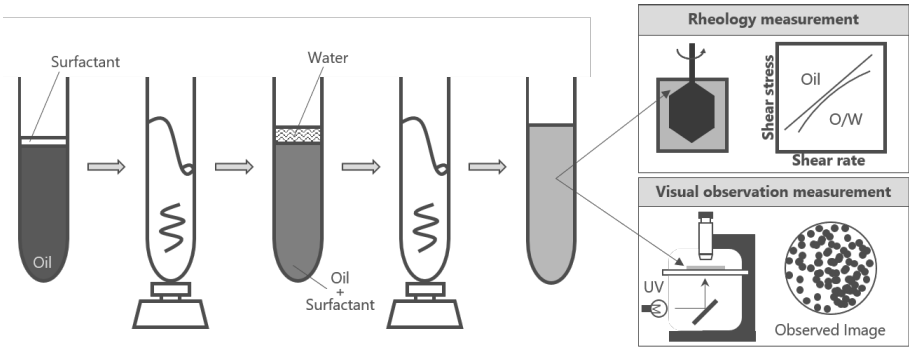

Figure 2 Schematic diagram of experimental procedure.

Table 1 Test sample conditions

Case #	Chemical agent	Description	Conc. of C.A.[1)]	Oil	Water fraction
1	-	Control sample without additive	-	Heavy fuel oil (Ref. to Fig.1)	0~50%
2	NEOS AB3000[2)]	Commercial oil dispersant	10%		
3	NIKKOL OPT-75[3)]	Diethylhexyl sodium sulfosuccinate 75% solution diluted by water and ethanol (HLB>20)	2%		
4	NIKKOL MYL-10[4)]	PEG-10 laurate (HLB=12.5)	1%		
5			2%		
6			4%		

1) Concentration of the chemical agent is defined as weight ratio relative to the oil.
2) https://www.epa.gov/emergency-response/neos-ab3000
3) https://www.chemical-navi.com/product-search/en_view3575.html
4) https://www.chemical-navi.com/product-search/en_view282.html

2.2. Viscosity Measurement

The prepared test samples were measured for viscosity characteristics using the B-type viscometer described above. An example of the measurement is shown in Fig.3 , which gives the relation between shear rate and shear stress at a certain water fraction ϕ_w. As seen in this figures, the emulsified sample becomes a non-Newtonian fluid so that the viscosity changes depending on the shear rate, thus the shear rate of 100.44 1/s is selected to define the representative viscosity in the following discussions.

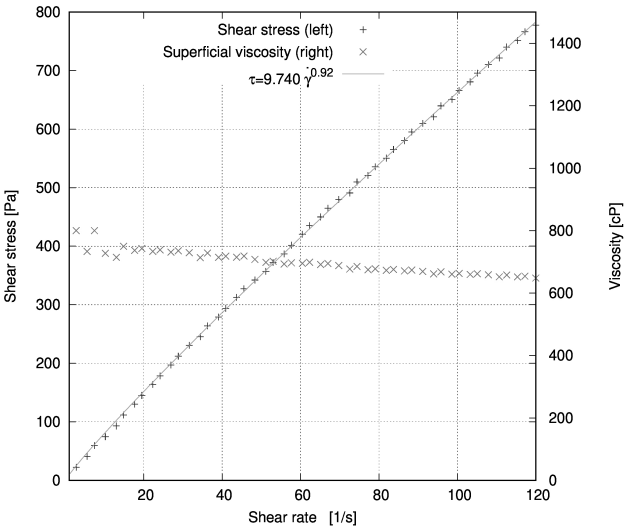

Figure 3 Example of viscosity measurement
Case 2 and $\phi_w = 0.154$

Experimental results of viscosity measurement in this study are given in Fig.4. The horizontal axis is the volume fraction of water added, and the vertical axis is the viscosity normalized by the initial viscosity without water addition. First, we look at Case 1, which does not contain any chemical agent. In this case, as the amount of water added is increased, the viscosity of the emulsion increases. This trend continues up to the limit of water addition where the entire system can be treated as a uniform emulsion with no water separation phase.

On the other hand, in the cases with additive (Case 2 to Case6), quite different behavior was observed. At the beginning when the water fraction was small, the viscosity increased with the addition of water as same as seen in Case 1. However, if the amount of water was further increased, the viscosity decreased suddenly and sharply at a certain point.

This sudden drop in viscosity was a remarkable characteristic that was observed only in the cases with additives as not seen in the case where additive absent (Case 1), and also seemed to imply that some rheological phase transition took place. Comparing the case 2,3 and 5, the critical value of the water fraction at which the viscosity drop occurred depended on the type of additive.

The viscosity drop also depended on the concentration of the additive. Case 4 to 6 with the same surfactant had the critical water fraction ranged from 0.18 to 0.28. Increasing the concentration of surfactant caused the drop with a smaller amount of water addition. When the water is added further after a discontinuous viscosity drop occurs, the system still remains in an uniform emulsion state, and decreases its viscosity as the water addition increases.

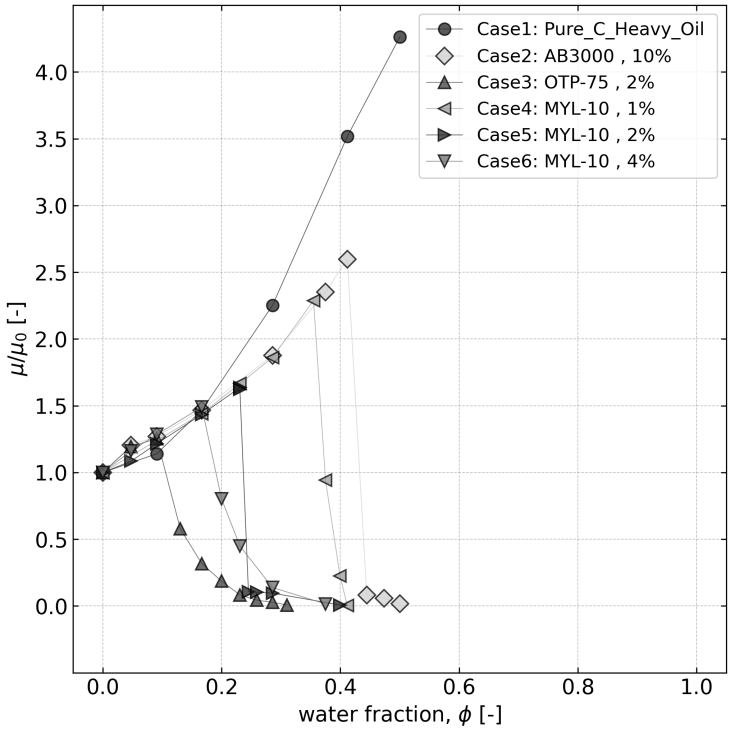

Figure 4 Viscosity profile of heavy fuel oil and water emulsion

2.3. Microscope Observation

In addition to the viscosity measurement, in order to understand the microscopic structure of emulsion, visualization observations were carried out using a UV fluorescence microscope (OLYMPUS BX50 System Microscope). Since oil fluoresces when exposed to ultraviolet rays, it is possible to determine whether the oil forms dispersed particles or a continuous phase. Figure 5 gives an example of Case 2. In this example, with a small amount of water added, water forms particlurate in the continuous oil media as shown on the left hand side. To the contrary, with a large amount of water added, oil forms particlurate in the continuous water media as shown on the right hand side.

The captured images were analyzed by image processing. The video data was decomposed into still images for subsequent image analysis. Each still image was converted to grayscale, and then binarized to calculate the ratio of the oil and water constituent areas. Since the particle distribution is not uniform, a small inspection window traverses the entire picture as shown in Fig.6. For the image processing, a free software named "OpenCV" was used (https://opencv.org/). The results of the image analysis were organized as a frequency distribution of oil fraction , then regressed to a following distribution function(Kanda J,1981):

$$f(x) = \frac{dF(x)}{dx} = \frac{d}{dx}\left[exp\left\{-\left(\frac{g-x}{\nu(x-a)}\right)^{\kappa}\right\}\right] \quad (1)$$

This distribution function is bounded both on the lower and upper side and defined in the support [a,g], which is suitable for representing the distribution of oil fraction by letting a and g be 0 and 1, respectively. Parameters ν and κ, which define scale and shape of the distribution, respectively, were determined from the image processing results by regression. An example is given in Fig.7. The results of the image processing will be used in the discussion in Chapter 4 .

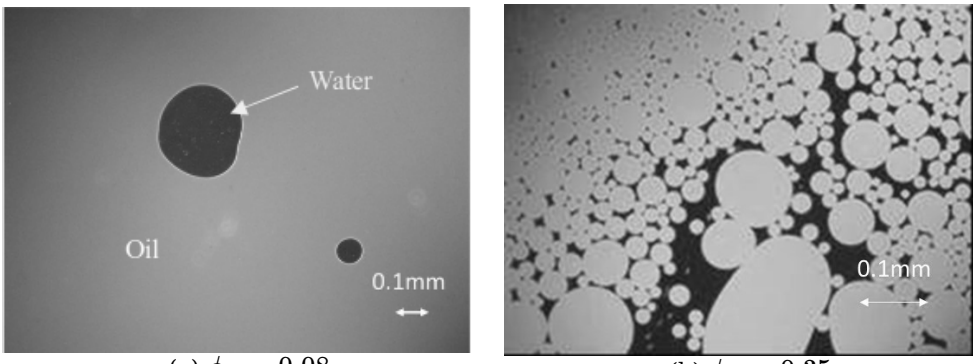

(a) $\phi_w = 0.08$ (b) $\phi_w = 0.35$

Figure 5 Example of fluorescence microscope observation
Case 2, AB-3000

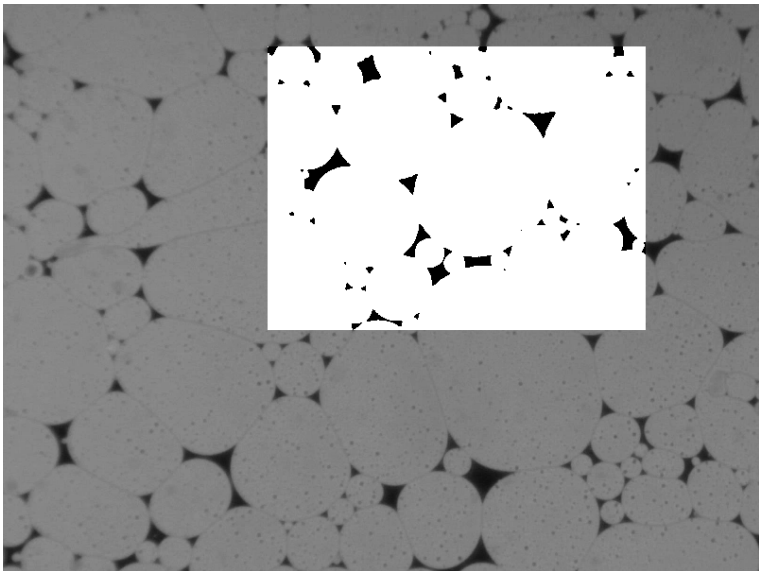

Figure 6 Image processing

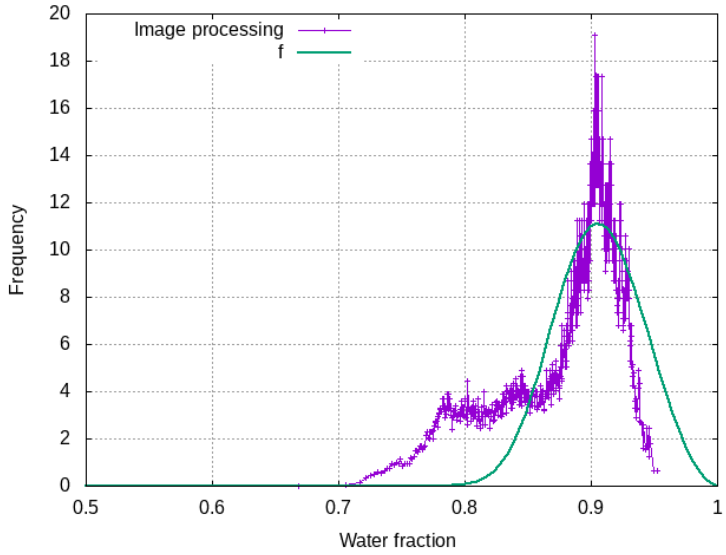

Figure 7 Oil fraction distribution obtained from image analysis
(Case 4: MYL-10 1% High viscosity region)

3. Viscosity model

In this chapter, we would like to develop a new viscosity model for oil-water (liquid-liquid) dispersed system. For solid-liquid dispersed system, namely suspension, there have been many models proposed so far. Einstein theorized the viscosity equation of suspensions, which is known to agree well with the measured value under low concentration conditions (A.Einstein,1906). Brinkmann et al. developed a viscosity prediction equation using Darcy's law for fluids flowing in porous media (H.C.Brinkmann,1949). Mori and Ototake developed a simple viscosity equation using the thickness of the liquid film between particles in a suspension (Y.Mori,1955). Their formulas are given in Table 2.

Table 2 Formulas of preceding works

Name	Equation	Eq. #
Einstein	$\mu_e = \mu_b \left(1 + 2.5\phi_p\right)$	(2)
Brinkmann	$\mu_e = \mu_b (1 - \phi_p)^{-2.5}$	(3)
Mori and Otoktake	$\mu_e = \mu_b \left\{ 1 + \frac{3}{\frac{1}{\phi_p} - \frac{1}{0.52}} \right\}$	(4)

In the solid-liquid suspension, solid material always forms dispersed phase, however, the liquid-liquid dispersed system, namely suspension, is a bit more complicated so that it depends on various condition whether a certain component may play as a dispersed phase or a continuous phase. As seen in the previous chapters, drastic viscosity drop was observed in the oil-water dispersion system. This observation may suggest that the structure of the dispersion system has changed significantly.

In this research, Fujita and Ma worked together to create an intuitive and concise model of the viscosity of a dispersed system that can include such a phenomenon. In this model, the dispersed system is hypothetically simplified as a stack of two layers , a layer densely packed with dispersed particles and a bulk layer without particles .

Referring to a schematic shown in Fig.8, the mathematical formulation is derived as follows. It is assumed that the two components, B and P, are mixed as a dispersed system as shown on the left side of the figure. Let us assume that component P constitutes particles. Our model considers the dispersed system to be equivalent to the stack of two layers as shown in the center of the figure.

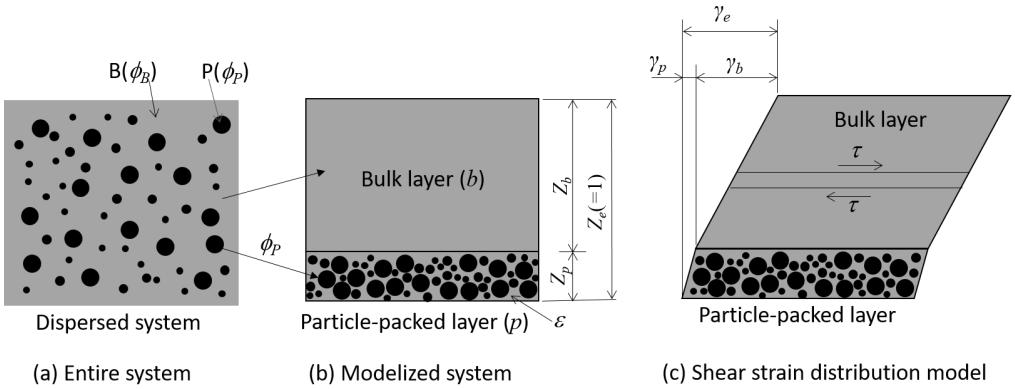

Figure 8 Schematic of layer-stacking model for liquid-liquid emulsion

In this layer-stacking model, letting the volume fractions of component B and component P be ϕ_B and ϕ_P, respectively, assuming that they are immiscible and there is no volume change due to mixing, the volume conservation gives:

$$\phi_B + \phi_P = 1 \tag{5}$$

As for the layer thickness, letting Z_p and Z_b be the fractions of layer thickness of the partilce-packed layer and the bulk layer, respectively, they satisfy:

$$Z_b + Z_p = 1 \tag{6}$$

It is assumed that all the P component is included in the particle-packed layer and packed as densely as possible. A new parameter ϵ is introduced to define the relationship between the volume fraction, ϕ_P, and the particle-packed layer thickness, Z_P , which is:

$$Z_p(1-\epsilon) = \phi_P \tag{7}$$

The parameter ϵ physically means a porosity, or a void fraction that the components other than P occupies in the particle-packed layer.

Next, in order to consider the viscosity, we give a shear deformation to the dispersed system. As shown on the right side of Fig. 5, the shear deformation is distributed to the bulk layer and the particle-packed layer. Let γ_e, γ_b and γ_p be the shear deformation of the entire layer, the bulk layer and the particle-packed layer, respectively, the shear deformation of the entire system should be the sum of the layers as follows:

$$\gamma_e = \gamma_b + \gamma_p \tag{8}$$

Shear stress τ is common to all the layers and can be described using shear strain $\frac{\gamma}{Z}$ and viscosity μ of each layer as follows:

$$\tau = \mu_e \dot{\gamma}_e = \mu_b \frac{\dot{\gamma}_b}{Z_b} = \mu_p \frac{\dot{\gamma}_p}{Z_p} \tag{9}$$

, where dot means time derivative. Let us define β_b as a ratio of bulk layer deformation to the entire shear, which is:

$$\beta_b = \frac{\gamma_b}{\gamma_e} \tag{10}$$

By applying Eqs.(10),(7) and (6) to Eq.(9), the viscosity of the entire dispersed system can be evaluated using only the viscosity of the bulk layer as follows:

$$\mu_e = \mu_b \frac{1}{Z_b}\frac{\dot{\gamma}_b}{\dot{\gamma}_e} = \mu_b \frac{1}{Z_b}\beta_b = \mu_b \beta_b \frac{1-\epsilon}{1-\epsilon-\phi_P} \tag{11}$$

When ϕ_P is small ($\phi_P \to 0$), using the Taylor expansion, Eq.(11) can be linearized with respect to the volume fraction ϕ_P, giving the following equation:

$$\mu_e = \mu_b \beta_b \left(1 + \frac{1}{1-\epsilon}\phi_P\right) \tag{12}$$

As for the deformation ratio β_b, considering the particle-packed layer to be less deformable than the bulk layer, and also the limit where the ϕ_P approaches 0, β_b is expected to be a function that asymptotically approaches 1 like:

$$\beta_b = 1 - \beta_p = 1 - \frac{\gamma_p}{\gamma_e} = 1 - Z_p f(\dot{\gamma}_e) = 1 - \frac{\phi_p}{1-\epsilon} f(\dot{\gamma}_e) \tag{13}$$

, where $\beta_p = \frac{\gamma_p}{\gamma_p}$ is strain leakage to the particle-packed layer, and $f(x)$ is a monotonically increasing function that takes 0 at $x = 0$ and has an upper bound less than or equal to 1.

In deriving this equation, we assume that the particle-packed layer has its deformation proportional to the layer thickness, but it is immobilized when the strain rate is small while it can move to some extent as the stain rate increases. This model is hypothetical, but if accepted, it could explain the pseudoplasticity observed in W/O emulsions, as shown in Fig.9. This example is given for a fluid of $\tau \propto \dot{\gamma}_e{}^{0.8}$ by letting f be a expression for the first-order relaxation phenomenon as:

$$f(\dot{\gamma}_e) = f_0 \left\{1 - exp(-\frac{\dot{\gamma}_e}{\dot{\gamma}_0})\right\} \tag{14}$$

, which makes you see the model has good representation for the pseudoplasticity. It should be noted that, in the following chapter, we neglect the effect of shear strain rate and let $\beta_b = 1$, since the main discussion is developed at the fixed strain rate.

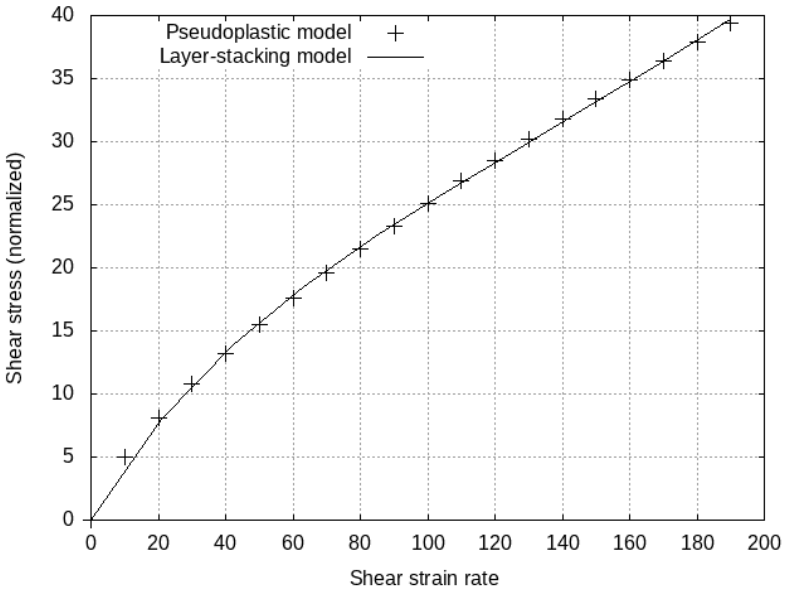

Figure 9 Example of layer-stacking model applied to pseudoplastic fluid

On the other hand, ϵ, the parameter related to the porosity in the particle-packed layer, may change variously depending on the conditions. In special case when the particle size is constant, Kepler conjecture, a mathematical theorem about sphere packing in three-dimensional Euclidean space, gives an upper limit for ϵ, which is about 0.26. Einstein's model (2) has its coefficient 2.5 which can be interpreted as ϵ of 0.6 in the layer-stacking model. For example, viscosity change predicted by the layer-stacking model is given by Fig.10. Two typical cases are plotted which are $\epsilon = 0.26$ for the Kepler limit and $\epsilon = 0.6$ for Einstein model.

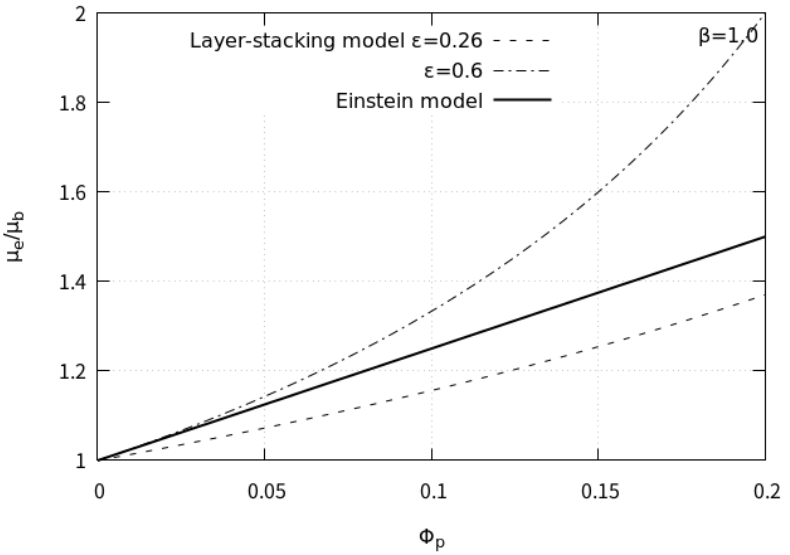

Figure 10 Viscosity change predicted by layer-stacking model

In the above derivation, the component P was treated as forming particles in the particle-packed layer, however, in case of multiple emulsion as shown in Fig.11, the component P may become a liquid that fills the void in the particle-packed layer. Even in this case, Eqs. (11) and (12) are still valid by changing the interpretation of the porosity, ε, to the volume fraction of particles constituted by component B. The layer-stacking model asserts that the viscosity of the entire system depends on the thickness and properties of the bulk layer, and ε can be interpreted as a parameter that represents the amount of bulk layer components taken up by the particle-packed layer. ϵ is alwasys filled with bulk component. In that sense, from here on, ϵ should be written as ϵ_b or ϵ_B.

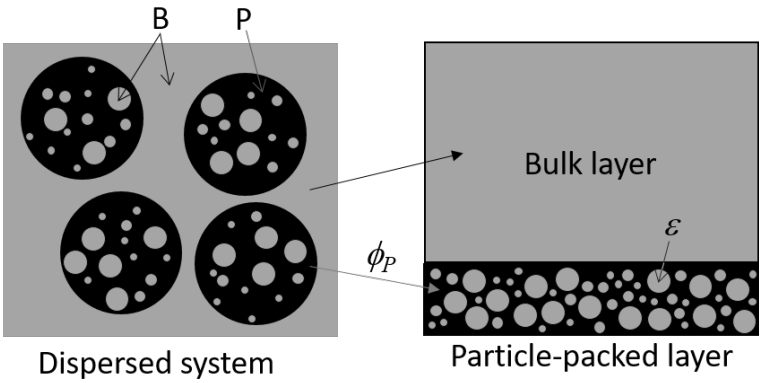

Figure 11 Schematic of layer-stacking model for multiple emulsion

To summarize this chapter, we introduced a simple layer-stacking model, which divides the dispersed system into a particle-packed layer and a bulk layer. In this model, the entire viscosity of the dispersed system is determined by the attributes of the bulk layer of its viscosity and thickness.

4. Discussions

In this chapter, we discuss the viscosity characteristics of oil-water emulsion system observed in the experiment results described in Section 2.2 In particular, we focus on the continuous viscosity change and discontinuous and sudden viscosity drop. For the discussion, we will use the layer-stacking model introduced in Chapter 3 and the results of image analysis of microscopic observation introduced in Section 2.3.

When the water addition, ϕ_w, is small, the oil component constitutes the bulk layer. In this case, the layer-stacking model, Eq.11, assuming that $\beta = 1.0$, gives the viscosity of the entire system(μ_e) normalized by the oil viscosity(μ_o) as:

$$\frac{\mu_e}{\mu_o} = \frac{1-\epsilon_o}{1-\epsilon_o-\phi_w} \tag{15}$$

, where ϕ_w is a volume fraction of water added to the entire system, and ϵ_o is a volume fraction that oil component occupies in the particle-packed layer which is determined by a least square curve fitting with the experimental data. Curve fitting results are given in Fig.12 for the case 1 to 6. In the figures, other models by Einstein (Eq.2), Brinkmann (Eq.3) and Mori and Otokake (Eq.4) are also plotted. Adjusting the parameter, ϵ_o, to the appropriate values, the layer-stacking model has better representation of the experimental data than the other models. In this experiment, values of 0.34 to 0.58 were obtained as ϵ_o depending on each case. The larger the ε, the larger the increase rate of viscosity, but in the cases of 2 to 6 containing the surfactant, it was found that the larger the ϵ, the faster the system jumps to the low viscosity region with respect to the water addition as shown in Fig.13. This seems to suggest a relationship between ϵ and the stability of the system, which will become clearer in the following discussion on the region where water addition is large.

To the contrary, when ϕ_w is larger than the critical value, water constitutes the bulk layer. In this case, the layer-stacking model can be written as:

$$\frac{\mu_e}{\mu_w} = \frac{1-\epsilon_w}{\phi_w-\epsilon_w} \tag{16}$$

This equation has a singularity at $\phi_w = \epsilon_w$, and diverges to infininty when ϕ_w approaches ϵ_w, which seems to provide physical insight into the stability of the system. The emulsion which has water as a bulk layer is only stable when the water fraction is in the range $[\epsilon_w, 1]$, and when the water fraction falls below ϵ_w, the system becomes unstable so as to trigger phase inversion.

This hypothesis will be tested using experimental data. As shown in Fig. 8, the intersection of the line obtained by regressing the data in which the viscosity drop took place by Eq. (12) and the regression line in which the viscosity drop did not occur seems to coincide with the critical point where the viscosity drop takes place.

If we draw the lines of equations (14) and (15), we obtain a region that overlaps the allowable water content, as shown in Fig.14. Within this region, it seems that both states can exist. However, in our experiments, emulsions with water as the continuous phase were generated in the overlapping region. This may depend on the thermodynamic free energy, and in this region, it is conceivable that the state in which water forms a continuous phase has a smaller energy than the state in which oil forms a continuous phase, although we cannot say for sure because emulsions are not thermodynamically stable systems.

As a guideline for future development, in order to reduce the viscosity with as little water as possible, it is important to make the ϵ_w as small as possible, that is, to form the particle-packed layer as densely as possible as the structure of the emulsion. However, when the diameter of the dispersed particles is constant, ϵ_w is limited by Kepler conjecture. If the particle size is various so that small particles fill the gaps between large particles, or if the particles are not spherical, it may be possible to overcome the Kepler conjecture limit. In this experiment as well, in cases 3, 5 and 6, ϵ_w was obtained to be lower than Kepler's conjecture.

Next, we discuss the microscopic structure of emulsions. When no chemical agent is added, the structure of emulsions formed in an oil-water system is relatively simple to be an water-in-oil (W/O) emulsion, while emulsions formed in a system with chemical agent can have a complex structure. Figure 15 shows the fluorescence microscope observation of the structure of oil and water in a particle-packed layer. The figure includes two cases, Case 3 and 5. For each case, series of images with different water fraction are given. Images with a picture frame are the observation in the high-viscosity region, and images without a picture frame were taken in the low-viscosity region. In

Case 3, it was observed that particulates were formed by oil in the low-viscosity region and water in the high-viscosity region, respectively. This means that in Case 3, the emulsion system changes its form from W/O emulsion to O/W emulsion with increase of water addition. On the other hand, in Case 5, particulates were formed by oil in both of the low-viscosity region and the high-viscosity region, which means that the system has O/W/O multiple emulsion in the low-viscosity region and changes its form to O/W emulsion. Although the structure of the emulsions changes depending on the type of chemical agent, the layer-stacking model can explain them comprehensively.

Finally, we examined the agreement between the area of oil or water obtained from the image processing and the ϵ obtained from the model fitting. Case 3 is shown in Fig.16 as an example. The image on the left is the one taken in the high viscosity region, giving ϵ_o of 0.68, and the image on the right is taken in the low-viscosity region, giving ϵ_w of 0.13. These values obtained from image analysis do not necessarily have to match those obtained from model fitting. In fact, in the high viscosity region, the values obtained from model fitting and image processing has some discrepancy: 0.58 for model fitting and 0.68 for image processing. On the other hand, in the low-viscosity region, the model fitting and image processing gave values of 0.13 and 0.13, respectively. As for the other cases, results are summarized in Table 3. Observing other cases as well, there is a quantitative discrepancy between the ε obtained by image processing and that of model fitting. However, comparing cases 4-6, where MYL-10 was used as the surfactant, as the surfactant concentration increases, ϵ_o increases in the high viscosity region, while ϵ_w decreases in the low viscosity region. This trend is common to both image processing and model fitting. This finding implies that the parameter, ϵ, in the model, even though having been introduced hypothetically at first, may represent the actual physical structure qualitatively.

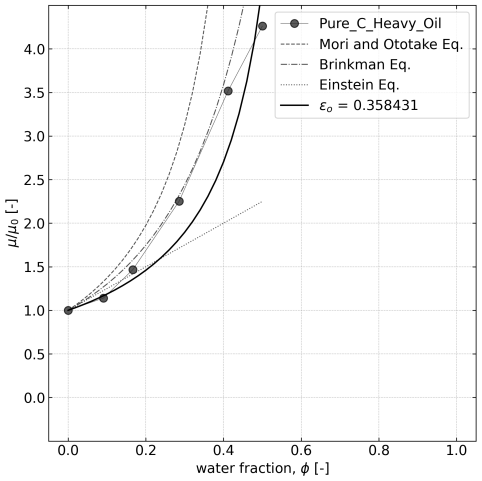

(a) Case1: C heavy oil

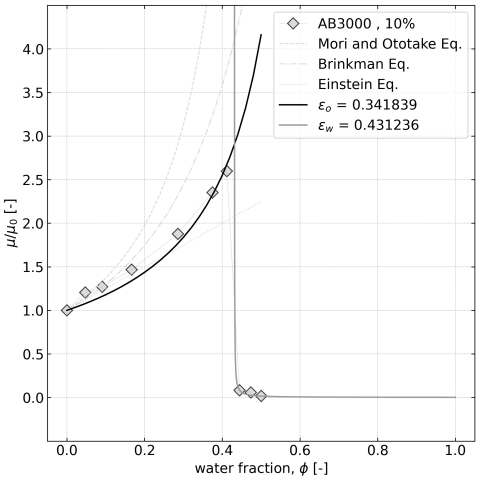

(b) Case2: AB3000, 10%

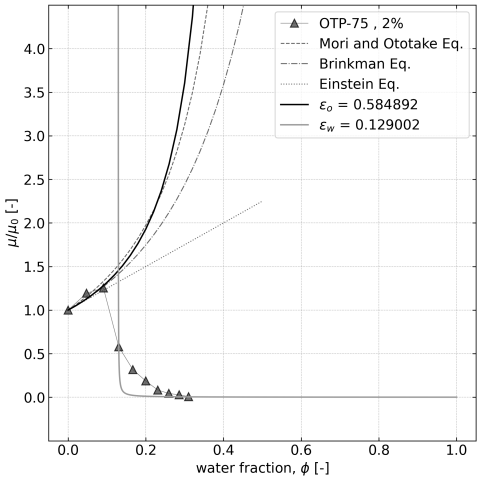

(c) Case3: OTP75, 2%

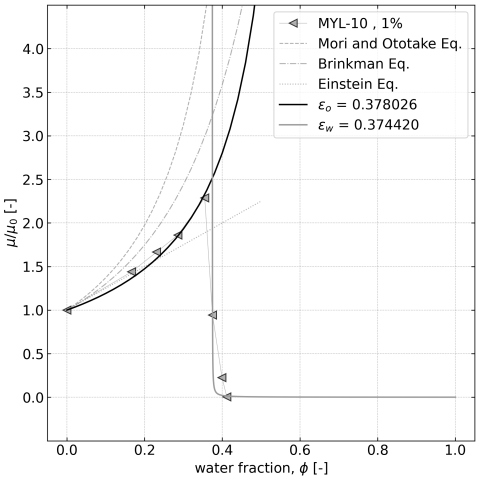

(d) Case4: MYL10, 1%

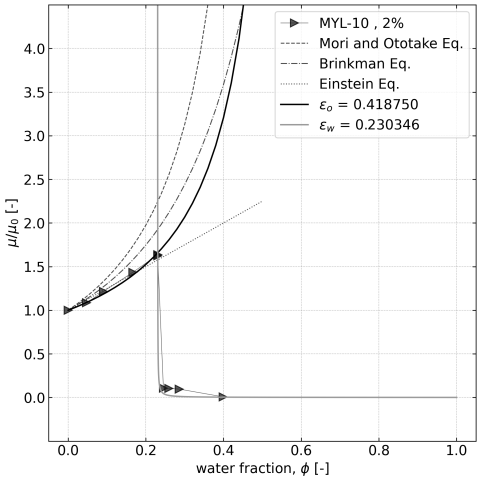

(e) Case5: MYL10, 2%

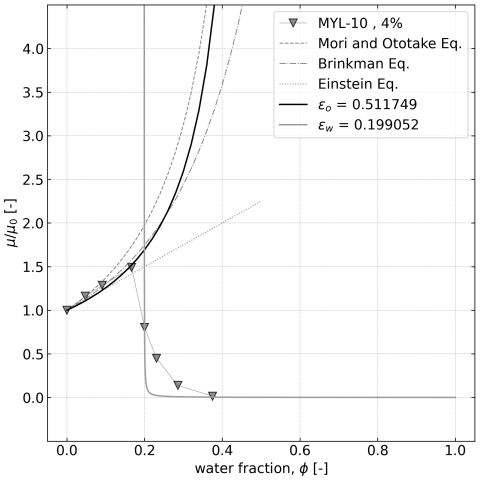

(f) Case6: MYL10, 4%

Figure 12 Measured viscosities and Layer-stacking model fitting

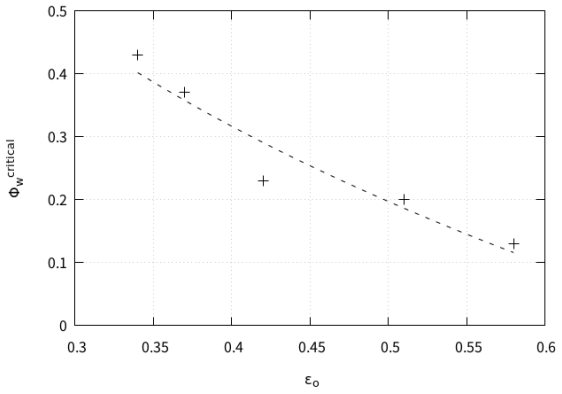

Figure 13 Relation between ϵ_o and the critical water addition ratio

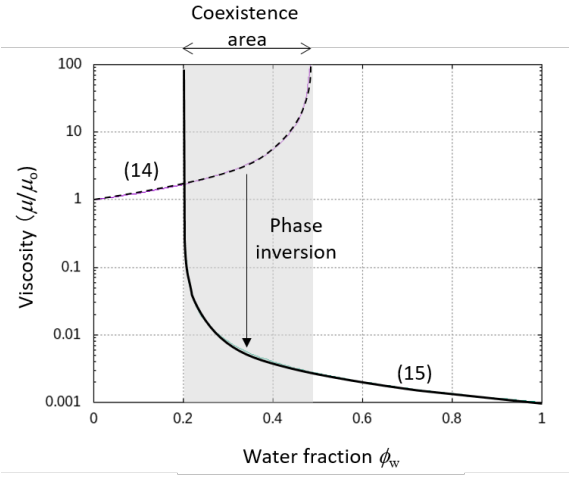

Figure 14 Schematic diagram of phase inversion

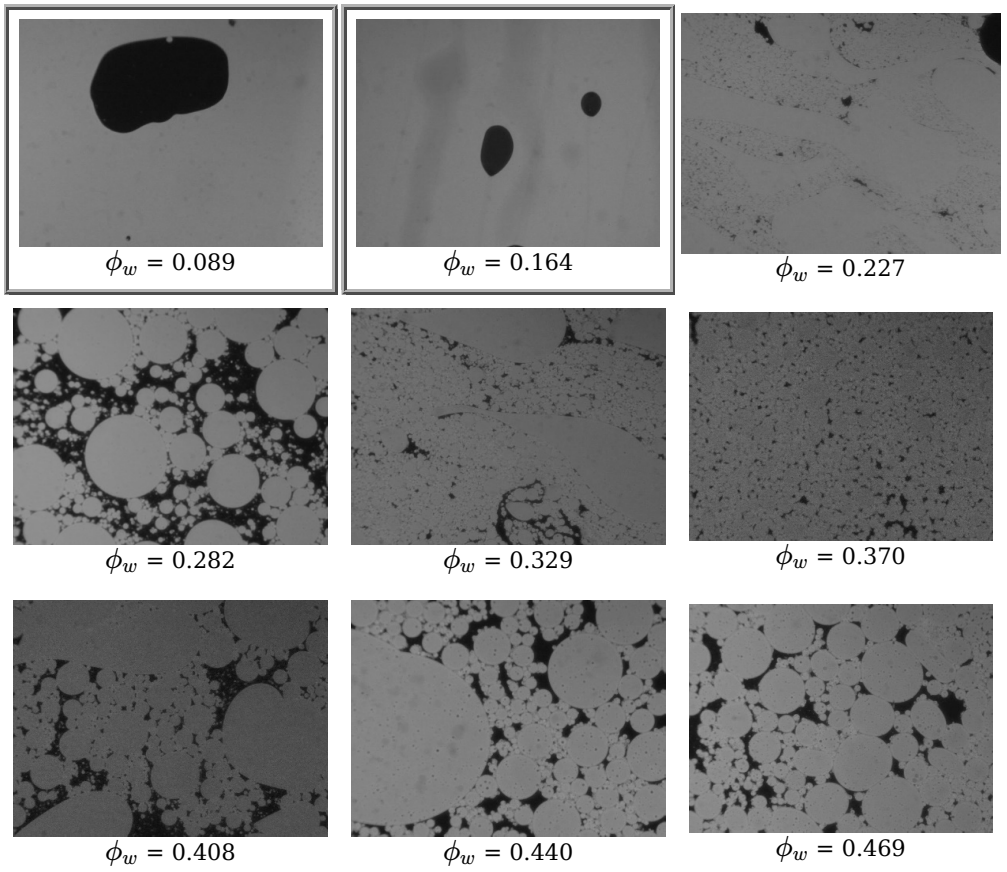

(a) Case3: OTP75-2%, x20.

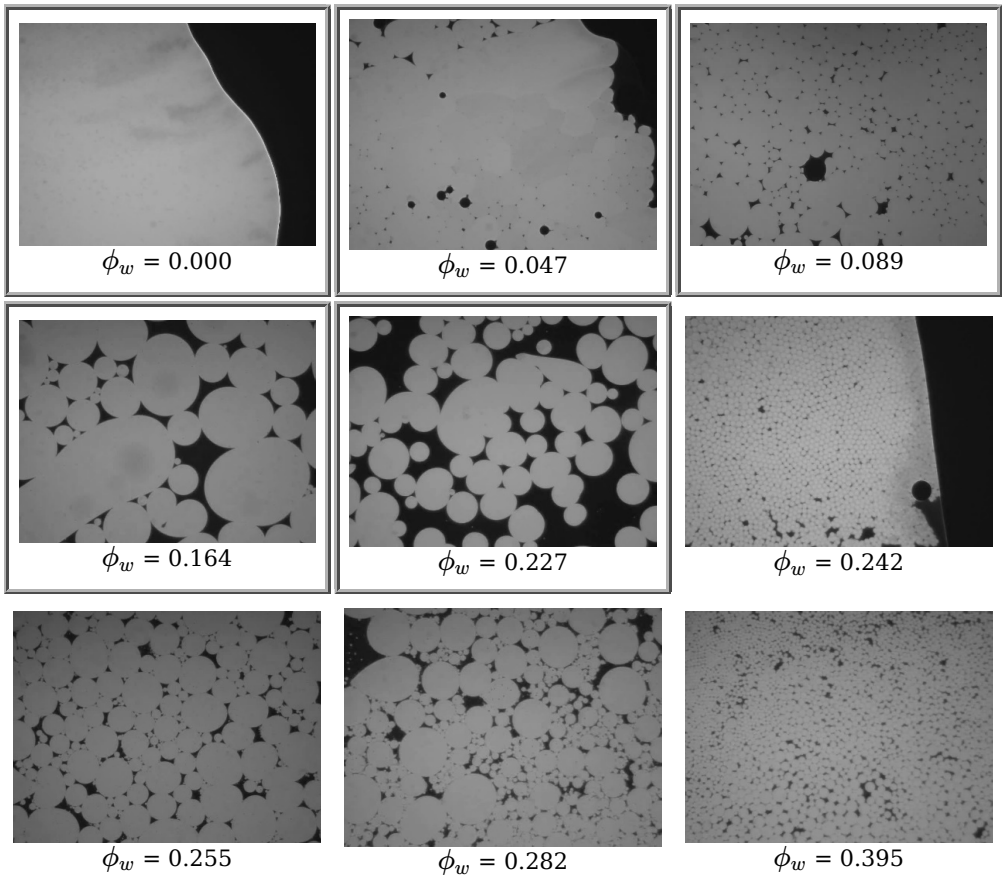

(b) Case 5: MYL10-2%, x20.

Figure 15 Observed results by fluorescence microscope.
(Images with picture frame are in high-viscosity region,
and others are in low-viscosity region)

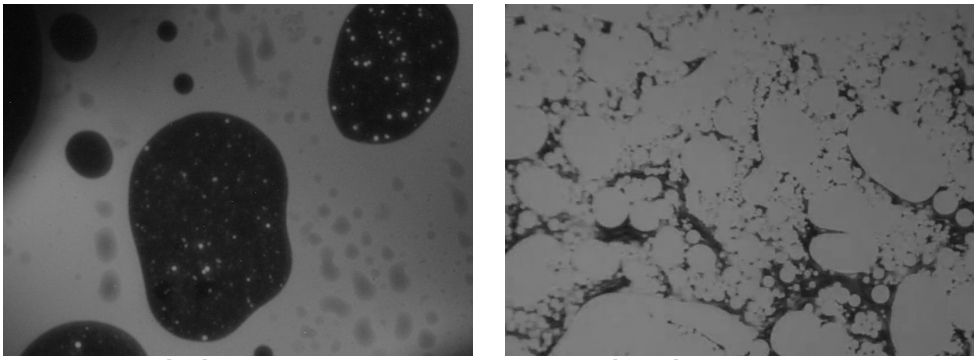

(a) In high-viscosity region $\epsilon_o = 0.68$ (b) In low-viscosity region $\epsilon_w = 0.13$

Figure 16 Microscope image used for image processing
(Case 3, OTP-75 2%)

Table 3 Comparison of $\epsilon_{o/w}$

Case #	Chemical agent	High viscoisty region ϵ_o		Low viscoisty region ϵ_w	
		Image proc. (Min./Median/Max.)*	**Model fit.** (Eq.15)	**Image proc.** (Min./Median/Max.)*	**Model fit.** (Eq.16)
1	none	0.491 / 0.814 / 0.993	0.358	N/A	N/A
2	AB3000	0.753 / 0.891 / 0.983	0.341	0.010 / 0.052 / 0.114	0.431
3	OTP-75	0.559 / 0.884 / 0.996	0.58	0.009 / 0.107 / 0.304	0.129
4	MYL-10 (1%)	0.772 / 0.878 / 0.970	0.378	0.001 / 0.047 / 0.236	0.374
5	MYL-10 (2%)	0.723 / 0.914 / 0.994	0.418	0.003 / 0.033 / 0.09	0.230
6	MYL-10 (4%)	0.846 / 0.965 / 0.998	0.511	0.000 / 0.013 / 0.073	0.199

* Min./max. are defined as values that covers 95% (2σ coverage in normal distribution) with the median value in the middle.

5. Conclusions

In this paper, emulsions of heavy fuel oil and water were investigated. In the experiments, oil/water emulsions with surface active agents were prepared to measure their viscosity characteristic and observe their microscopic structure using fluorescence microscope. In the theoretical analysis, a new layer-stacking model was proposed to compare and interpret the experimental results. The following findings were obtained:

- In the region of low water content, the viscosity of oil-water emulsions increases with increasing water content.
- In the system with surfactant, the viscosity suddenly decreases when the water content reaches a certain critical value caused by phase inversion.
- The newly introduced layer-stacking model can well represent the increasing viscosity characteristics of emulsions.
- The layer stacking model introduced a new parameter defined as a fraction of the continuous phase component in the particle-packed layer. This parameter is related to the stability of the emulsion system and can explain the viscosity drop triggered by the phase inversion.
- Microscopic observations corroborate the above results.

Acknowledgments

This work was funded by JSPS KAKENHI Grant Number JP19K04870. Nikko Chemicals Co., Ltd. kindly provided us with a sample of surfactant. Dr. Kuwae, group leader of Coastal and Estuaries Environment Research Group of Port and Airport Research Inst. , kindly let us use the expensive fluorescence microsope with no compensation. Dr. Taku Ogura, a visiting Associate Professor of Tokyo University of Science gave us valuable advices. We would like to express our gratitude by writing here. Last but not least, we will present this paper as a sincere condolence and acknowledgement to our long-time colleague, Dr. Shoichi Hara, who led us to this topic

in the beginning of this research.

References

A. Einstein, "Eine neue Bestimmung der Moleküldimensionen," *Annalen der Physik*, 324,2 (1906)

Bannwart A.C., Rodriguez Oscar M., Carvalho Carlos, Wang Isabela and Vara Rosa, "Flow Patterns in Heavy Crude Oil-Water Flow," *Journal of Energy Resources Technology-transactions of The Asme - J ENERG RESOUR TECHNOL*, DOI:10.1115/1.1789520 (2004)

Drieu Commander, MacKay Ron, Hvidbak Flemming, Nourse Lieutenant and Cooper David, "Latest Update of Tests and Improvements to Coast Guard Viscous Oil Pumping System (VOPS) 1," *International Oil Spill Conference Proceedings volume=*, undefined (2003)

H.C.Brinkmann, "A CALCULATION OF THE VISCOUS FORCE EXERTED BY A FLOWING FLUID ON A PHASE SWARM OF PARTICLES," *Appl. Sci. Res.*, A1 (1949)

Hansen Kurt, Guidroz Leo, Hazel Bill, Fitzpatrick Michele and Johnson Gregory, "Sunken Oil Recovery System Recommendations," *International Oil Spill Conference Proceedings 2014*, DOI:10.7901/2169-3358-2014.1.2014 (2014)

Isamu FUJITA and Yoshitaka MATSUZAKI, "Rheological Behavior of W/O Emulsion of Water-Heavy Oil System and Friction Loss Reduction Methods for its Flow in a Pipe," *PARI Report*, 052-04-03 (2013)

Isamu FUJITA, Kenji TAKEZAKI, Yoshitaka MATSUZAKI, Yoshirou KATO and Keiji KAKIZAKI, "Friction Loss Reduction by Water Injection in Pipe Line Flow of Heavy Oil Emulsion," *Annual Journal of Civil Engineering in the Ocean, JSCE*, 25 (2009)

Isamu FUJITA, Yoshitaka MATSUZAKI and Tetsuya SHIRAISHI, "Friction Loss Control of Heavy Oil Emulsion in Pipe Line by Surface Active Agents," *J. JSCE*, 67, 2 (2011)

Kanda J, "A New Extreme Value Distribution with Lower and Upper Limits for Eathquake Motions and Wind Speeds," *Proc. of the 31st Japan National Congress for Applied Mechnics*, pp.351-360 (1981)

M. Ono, H. Shirota, I. Fujita, S. Hara and O. Miyata, "Study on Refinement and Fluidization of High Viscosity Oil by Pressure Wave," *Proc. 27 th Ocean Engineering Symposium*, OES27-030 (2018)

M. Ono, O. Miyata, S. Hara, H. Kifune and S. Shimonishi, "Oil recovery method from a simulated tank of a real ship using electromagnetic induction heating," *Proc. 25 th Ocean Engineering Symposium*, OES25-056 (2015)

M. Ono, O. Miyata, S. Hara, H. Kifune, S. Shimonishi and H. Kagemoto, "Technology for countermeasures against oil spills from sunken ships," *Proc. 15 th NMRI Symposium*, PS-20 (2015)

M.Ono, H.Shirota, S.Hara, O.Miyata, I.Fujita and H.Kifune, "Method and system for treatment of high-viscosity oil (in Japanese)," *JP patent*, #6748386 (2019)

Russell.T.W.F. and Charles,M.E., "The Effect of the Less Viscous Liquid in the Laminar Flow of Two Immiscible Liquids," *Can. J. Chem. Eng.*, 37, 18 (1959)

Vuong Duc, Zhang Hong-Quan, Sarica Cem , Li Mingxiu, "Experimental Study on High Viscosity Oil/Water Flow in Horizontal and Vertical Pipes," *proceedings - SPE Annual Technical Conference and Exhibition*, 4. 10.2118/124542-MS (2009)

Y. Mori and N. Ototake, "On the Viscosity of Suspensions," *Jpn. J. Chem. Eng.*, 20,9 (1955)